

ELASTIC PROPERTIES OF RELAXED, ACTIVATED, AND RIGOR MUSCLE FIBERS MEASURED WITH MICROSECOND RESOLUTION

D. W. G. JUNG, T. BLANGÉ, H. DE GRAAF, AND B. W. TREIJTEL
*Department of Physiology, University of Amsterdam, Meibergdreef 15,
1105 AZ Amsterdam, The Netherlands*

ABSTRACT Tension responses due to small and rapid length changes (completed within 40 μ s) were obtained from skinned single-fiber segments (4- to 7-mm length) of the iliofibularis muscle of the frog incubated in relaxing, rigor, and activating solution. The fibers were skinned by freeze-drying. The first 500 μ s of the responses for all three conditions could be described with a linear model, in which the fiber is regarded as a rod composed of infinitesimally small identical segments, containing an undamped elastic element, two damped elastic elements and a mass in series. An additional damped elastic element was needed to describe tension responses of activated fibers up to the first 5 ms. Consequently phase 1 and phase 2 of activated fibers can be described with four apparent elastic constants and three time constants.

The results indicate that fully activated fibers and fibers in rigor have similar elastic properties within the first 500 μ s of tension responses. This points either to an equal number of attached cross-bridges in rigor and activated fibers or to a different number of attached cross-bridges in rigor and activated fibers and nonlinear characteristics in rigor cross-bridges. Mass-shift measurements obtained from equatorial x-ray diffraction patterns support the latter possibility.

INTRODUCTION

The sliding-filament concept is based on the assumption that muscle shortening is the result of myosin and actin filament sliding, which is due to cross-bridge attachment and detachment. Isometric tension will develop if the muscle is prevented from shortening. Fast changes in tension responses of isometric muscle fibers, after fast length changes, can reflect cross-bridge behavior before attachment or detachment occurs.

Ford et al. (1977) divided tension transients of activated intact fibers, following a length change completed within 200 μ s, into four phases. The first two phases covered the first few milliseconds of the responses. More recently, Blangé and Stienen (1985*b*) used displacements with a much faster time course (completed within 50 μ s), which allowed them to resolve more details in the first two phases of tension responses of activated and relaxed frog muscle fibers. They could describe the first 100 μ s of these fast tension changes of activated and relaxed fibers with a model in which the fiber was regarded as a rod composed of infinitesimally small segments containing an undamped elastic element, a damped elastic element, and a mass in series. It was concluded that a very fast relaxation time (between 5 and 15 μ s) must be present in activated and relaxed fibers during phase 1.

Here, we give a complete model description of the first 2 (or 5) ms of tension responses of activated, rigor, and

relaxed skinned single-muscle fibers. This part of tension responses corresponds roughly with phase 1 and 2 of Ford et al. (1977) and reflects cross-bridge behavior just before attachment or detachment of cross-bridges occurs (Ford et al., 1974). The first 2 ms of tension responses of relaxed fibers and fibers in rigor (after small length changes completed within 40 μ s) can be described with a model containing an undamped elastic element and two damped elastic elements in series. With the same model one can describe only the first 500 μ s of tension responses of fully activated fibers (Blangé and Stienen, 1985*a*). Analysis of such tension recordings up to 5 ms indicates that an additional damped elastic element is needed for a satisfactory model simulation.

The values of the model parameters in the three states (activated, relaxed, and rigor) will be compared, in order to interpret the mechanical results in terms of cross-bridge properties and numbers of attached cross-bridges. Equatorial x-ray diffraction patterns, obtained from single fibers and fiber bundles, give information about the mass associated with the actin and myosin filament. The mass distribution gives additional information about the number of cross-bridges in activated and rigor fibers in the case of similar cross-bridge orientation and properties in these two states. Results from these equatorial measurements will be compared with the mechanical results.

Previous work has shown that freeze-dried frog muscle fibers are suitable preparations for the above mentioned

experiments (Blangé and Stienen, 1985b). Stienen et al. (1985) investigated the influence of Dextran and sarcomere length changes on the Ca^{2+} sensitivity of these fibers. Stienen and Blangé (1985) measured T_1/T_0 and T_2/T_0 curves (obtained from tension responses after length changes completed within 50 μs and 150 μs) as well as the speed of the fast recovery phase. They concluded that their results were similar to results obtained from intact fibers (Ford et al., 1977). ATPase activity of freeze-dried fibers has recently been measured by van der Laarse et al. (1986).

We will compare results obtained from freeze-dried fibers with those from Triton-treated fibers in order to illustrate that the observed mechanical fiber characteristics cannot be attributed to preparation artefacts.

Equatorial x-ray diffraction patterns of single fibers and fiber bundles support the observation that, with respect to filament spacing and mass distribution within the unit cell, freeze-dried fibers are similar to other skinned fibers or even intact fibers.

METHODS AND MATERIALS

Preparation

All of the mechanical and most of the x-ray measurements were performed on single muscle-fiber segments of the iliofibularis of the frog (*Rana esculenta*). The method of preparing these freeze-dried fibers is described by Stienen and Blangé (1985) and Stienen et al. (1983). Some of the x-ray results were obtained from bundles of freeze-dried muscle fibers. In two mechanical experiments we made use of chemically-skinned single-fiber segments. These fibers were skinned by means of the nonionic detergent Triton X-100, after a procedure similar to that used by Magid and Reedy (1980).

The length of the fiber segments ranged from 4 to 7 mm in the mechanical experiments and from 8 to 12 mm in the x-ray measurements. The single-fiber diameter varied between 100 and 200 μm . Fiber bundles had an average diameter of 300 μm .

Solutions

Here three types of solutions were used: relaxing, fully activating, and rigor solution. A computer program was used to calculate the free concentration of some important ions, pH, ionic strength, and the amount of KOH/HCl and KCl necessary to adjust pH and ionic strength of the solutions to the values desired at a chosen solution temperature. The program was based on that of Fabiato and Fabiato (1979). Several stability constants mentioned by Godt and Lindley (1982) were used. The actual amount of KOH/HCl necessary to adjust pH did not deviate more than 1 mM from the calculated amount. The temperature of the solutions was kept at $4.0 \pm 0.5^\circ\text{C}$. Table I summarizes the composition of the solutions.

Apparatus

The displacement generator used in the mechanical experiments is the one described by van den Hooff et al. (1982). The other devices that we used have been described by Stienen and Blangé (1985). In all mechanical experiments the sensitivity and natural frequency in air of the force transducer were 4.1 mV/mN and 55 kHz with noise of 5 μN . The natural frequency of the force transducer was between 50 and 55 kHz with the fiber mounted and placed in solution. The damping time constant of the force transducer was 150 μs . We did not try to damp the transducer because we preferred digital signal processing to mechanical signal

TABLE I
COMPOSITION OF THE INCUBATION SOLUTIONS

Solution	Relax	Rigor	Activation
Imidazol	60	60	60
EGTA	20	20	20
EDTA	—	5	—
CP	10	—	10
MgATP	5	—	5
Free Ca^{2+}	0	0	0.1
Free Mg^{2+}	1	0	1
Free Na^+	31	30	31
Free K^+	45	52	46
Free Cl^-	51	72	53

All concentrations of the three solutions are given in millimolar. Ionic strength 160 mM, pH 7.0 at 4.0°C . The relax and activation solutions contain 50 U/ml CK (creatine kinase). CP stands for creatine phosphate. (In two x-ray measurements chloride was exchanged by acetate).

processing. The tension and length changes were digitally recorded with a sampling rate of 2,000, 500, or 200 kHz.

Experimental Protocol

The freeze-dried fiber segments were mounted between the displacement generator and the force transducer with α -cyanoacrylate glue (Cyanolit 202, 3M Center, St. Paul, MN) in the dry state. Then the fibers were incubated in relaxing solution. The chemically-skinned fibers were mounted after incubation in the relaxing solution. This latter procedure resulted in some spreading of the glue along a certain length of the fibers. Other mounting procedures, such as clips or hooks, could perhaps prevent this problem but would introduce other experimental problems. The mounting procedure of the freeze-dried fibers avoided spreading of the glue; the glued fiber regions were well defined.

Sarcomere length was adjusted to 2.15 μm and checked in the relaxing solution by means of the diffraction pattern generated by a 5 mW He-Ne laser (wavelength: 632.8 nm; Spectra-Physics, Inc., Mountain View, CA).

The standard procedure in the experiments consisted of incubation in: relaxing solution (at least 5 min), low EGTA relaxing solution (5 min) with recording of tension responses to length changes, activation solution (~1 min) with recording of tension responses to length changes after development of a steady tension-level, relaxing solution (5 min) with recording of tension responses to length changes, rigor solution (5 min) with recording of tension responses to length changes after development of a steady tension-level. The low EGTA solution was similar to the relaxing solution, except that 20 mM EGTA was replaced by 0.2 mM EGTA and 19.8 mM HDTA (Moiescu and Thieleczek, 1978). Tension responses, obtained from fibers incubated in relaxing solution and in low EGTA relaxing solution, were identical.

During the procedure, fiber diameter and fiber length were measured (accuracy 5%) by means of a surgical microscope, without finding a systematic difference in fiber diameter during incubation in the three solutions. Uniformity of the sarcomere length over the fiber was inspected after each incubation in rigor and activation solution. Sarcomere length changes measured with laser-diffraction corresponded to the displacement of the tip of the displacement generator in all three solutions, as shown before for the activated fiber (Stienen and Blangé, 1985). Experiments were not continued if the steady isometric tension of a fiber upon activation decreased more than 5% of the tension at the beginning of the experiment, or if visible nonuniformities in the fiber developed.

Model

Model simulations were performed in order to characterize the measured tension responses in terms of elastic elements and damping coefficients.

Using a model based on the formalism described by Blangé and Stienen (1985b), we assumed that a single-fiber segment is a uniform rod of circular cross-section composed of small identical units connected in series with a density of 1,060 kg/m³. Each unit contains an undamped elastic element (E_1) and two damped elastic elements (elastic element E_2 , damping coefficient μ_2 , and elastic element E_3 , damping coefficient μ_3) in series.

An automated procedure, based on minimalisation of the mean square difference between the first 500 μ s of the measured tension response and the model-simulation, was used in order to estimate the five parameters of the model (E_1 , E_2 , E_3 , μ_2 , μ_3) for all measured tension responses of a fiber (data processing). In order to reduce variations in the parameter estimates due to noise and the resonant frequency of the force transducer, the digitally-recorded tension response and the recording of the length change (the input signal for the simulation procedure) were digitally filtered with a 20 kHz low-pass filter (30 times attenuation in the stop-band above 45 kHz). The linear phase (finite impulse response) filter was constructed by using a computer program of McClellan et al. (1973). Applied in this way the filtering procedure only prevents that the fitting procedure is dominated by the resonance of the force transducer or noise at high frequencies.

The simulations included the characteristics of the force transducer and corrections for effects due to the fluid surrounding the fiber (Blangé and Stienen, 1985b; Ford et al., 1977). Silicone rubber threads (diameter from 45 to 150 μ m) were used to test the calculated correction for surrounding fluid with different viscosities. The tension responses of these rubber threads to small length changes were fitted with the same model with which we described the tension responses of muscle fibers. Within experimental error the elastic parameters determined by the fitting procedure were independent of the viscosity of the surrounding fluid if the right viscosity value was incorporated in the fitting procedure, which suggests that the fluid correction is valid.

Figure 1 (right) shows typical effects of corrections, introduced for the characteristics of the force transducer and damping of the surrounding fluid. It could be confirmed, by means of measurements with different lengths of silk fiber, that instrumental delays were $<0.5 \mu$ s. However, in order to illustrate quantitatively the effects of supposed instrumental delays on the simulations, tension responses with different artificially-induced instrumental delays are shown in Fig. 5 (left) (see also Results).

The following formulas in Laplace transform notation were used for simulation:

$$T(s) = (-2kl) \cdot \{\exp(kl) - \exp(-kl)\}^{-1} \cdot f(s) \cdot Z(s) \cdot \epsilon(s) \quad (1)$$

$$k^2 = \{\rho_f s^2 + (4 \rho_m \eta R^{-2})^{0.5} s^{1.5} + \eta R^{-2} s\} / Z(s) \quad (2)$$

with ρ_m density and η viscosity of the surrounding fluid; ρ_f density, R radius of cross-section and l length of the fiber; $f(s)$ frequency characteristic of the force transducer; $\epsilon(s)$ input signal originating from the displacement generator; $Z(s)$ elastic impedance of the infinitesimal segment of the rod and $T(s)$ the calculated tension at the force transducer, i.e., the force, divided by the cross-sectional area πR^2 . See Blangé and Stienen (1985b) for a detailed explanation of these equations.

Apart from the data processing of tension responses of a fiber as it is described, the simulation procedure was performed on several tension responses of the fiber in the relaxed, activated, and rigor state, with fiber length as an extra variable parameter (formulas 1 and 2). Discrepancies between the fiber lengths determined in this way and the measured fiber length, would indicate that for some reason (e.g., inhomogeneity of the fiber or faulty measurement of fiber length or diameter) the model simulation did not suffice. The fiber lengths found by simulation were within the accuracy range of 5%, except for one experiment with a freeze-dried fiber, which was discarded, and the two experiments with the Triton-treated fibers. In the last two cases, the glue, which was used to mount the fiber, had spread along a certain length of the fiber. Therefore, in case of the Triton-treated fibers, parameters were not determined with

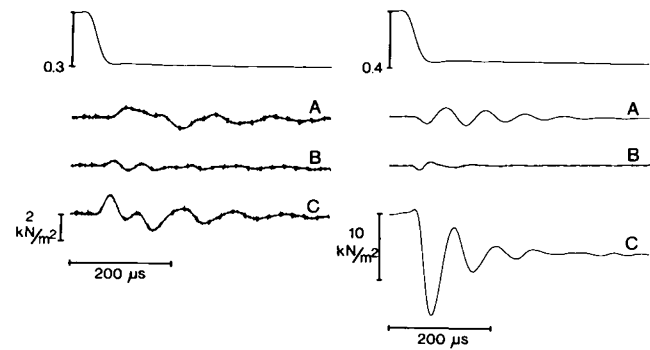


FIGURE 1 (Left panel) The difference between measured and simulated tension responses in case of artificially-induced instrumental delays. Simulations were obtained by demanding an overall optimal fit. In the simulations, the corrections for surrounding fluid and transducer characteristics are included. (Upper trace) Shortening of the fiber in nanometer/half sarcomere, (lower traces) difference signals in kN/m^2 . (A) difference between measured tension response (delay between onset displacement and start tension response changed by -5μ s) and optimal simulation; (B) difference between measured tension response (no change) and optimal simulation; (C) difference between measured tension response (delay between onset and displacement and start tension response changed by $+5 \mu$ s) and optimal simulation. Conditions: ionic strength 160 mM, pH 7.0, temperature 4.0°C , fiber length 7.0 mm, fiber diameter 135 μ , isometric active tension: 72 kN/m^2 , experiment: 27-03-1986 (Right panel) The amount of correction due to the fluid surrounding the fiber and the characteristics of the force transducer. (Upper trace) Shortening of the fiber in nanometer/half sarcomere, (lower traces) tension response and correction signals in kN/m^2 . Correction due to the fluid surrounding the fiber (A) and the characteristics of the force transducer (B) obtained by subtracting the model simulations with and without these corrections. (C) the corresponding measured rigor tension response, obtained after shortening of the fiber. Conditions: ionic strength 160 mM, pH 7.0, temperature 4.0°C , fiber length 5.6 mm, fiber diameter 180 μ , isometric rigor tension: 33 kN/m^2 , experiment: 07-11-1986.

the measured fiber length but with the fiber length estimated with the above mentioned simulations.

In those cases where the simulated and measured tension responses tended to deviate from each other after 500 μ s (on the 2 or 5 ms time scale), the five-parameter model was extended with another damped elastic element. This appeared to be necessary mainly in case of tension responses of activated fibers. Another automated procedure was then started to estimate the values of these seven model parameters. Consequently, activated fibers were in general simulated with the seven-parameter model, whereas relaxed fibers or rigor fibers were simulated with the five-parameter model.

X-ray Measurements

Equatorial x-ray diffraction patterns of activated, relaxed, and rigor single fibers and fiber bundles were obtained by making use of the small angle diffraction facility (beamline 7.2 and 8.2) of the Synchrotron Radiation Source at Daresbury (UK) (Nave et al., 1985). Muscle fibers and fiber bundles were mounted between mica windows in small perspex cells, the temperature of which could be controlled. The spacing between the windows was ~ 1 mm. The conditions and solutions were identical to those of the mechanical experiments, except that in two experiments chloride was exchanged by acetate in all solutions, without finding significant differences in the equatorial diffraction patterns. Sarcomere length was adjusted by means of laser diffraction. Tension exerted by the fibers was monitored continuously during the experiment.

The equatorial intensity was recorded with a linear position sensitive

detector under microcomputer control. Typical exposure times were 20 s for bundles and 20 to 60 s for single fibers. The data were transferred to a VAX 750 computer for least square analysis. No smoothing or averaging methods were used. The complete pattern on one side of the central beam was analyzed.

The background function used in the processing of the x-ray data was assumed to be of the form:

$$I(x) = a_1 + [a_2/(x - a_3)] + a_4 \cdot \exp\{-0.5[(x - a_3)/a_5]^2\} \quad (3)$$

which includes five adjustable parameters (a_i).

Five reflections have been taken into account, i.e. 10, 11, 20, 21, and the Z-line. The intensities of the peaks above background were defined as the areas under Gaussian peaks. The positions of the peaks were determined by the relation:

$$x_i = P_1 + \alpha_i \cdot P_2, \quad (4)$$

where $\alpha_i = 1$ for the 10 reflection, $\alpha_i = (3)^{0.5}$ for the 11 reflection, $\alpha_i = 2$ for the 20 reflection, and $\alpha_i = (7)^{0.5}$ for the 21 reflection corresponding to hexagonal symmetry of the filament lattice. For the Z-line α_i was taken to be 1.43, as found by Yu et al. (1985). For all measurements, P_1 was held fixed to the position of the central beam as obtained from the detector calibration. Accordingly, P_2 was the only variable position parameter in the least squares fit. The width of the peaks originating from the filament lattice, defined as the standard deviation of the Gaussians, could be fitted using a relation mentioned by Yu et al. (1985):

$$\sigma_i^2 = s_1^2 + \alpha_i^2 \cdot s_2^2 + \alpha_i^4 \cdot s_3^2 \quad (5)$$

s_1 was fixed at the width of the central beam leaving s_2 and s_3 as two independent line-width parameters for the filament lattice. The Z-line was not resolved in our experiments. However, in order to obtain satisfactory fits, it had to be included in the analyses. In some cases one variable parameter for the width of the Z-line yielded unrealistic results. Therefore, in these cases, the width of the Z-line was fixed to a realistic value, which was obtained by trial and error.

Masses associated with the actin and myosin filament were calculated from the Fourier projections. The calculations were made with the use of amplitudes of the 10 and 11 reflections. The relative amount of material in actin and myosin filaments expressed as a ratio A/M was calculated for two possible positions of the background. These values of A/M will be denoted as A/M(high)-background level on the lowest electron density value in the whole Fourier projection and A/M(low)-background level on the lowest electron density value along the line that joins the actin and myosin filaments (Haselgrove and Huxley, 1973).

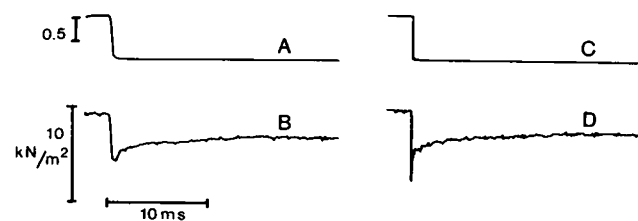


FIGURE 2 Tension transients of a single activated frog fiber to releases completed within 40 and 400 μ s on a 25-ms time scale. The length change is expressed in nanometer/half sarcomere, the tension responses in kN/m^2 . (A) Displacement signal, displacement completed within 400 μ s; (B) tension response of the activated fiber; (C) displacement signal, displacement completed within 40 μ s; (D) tension response of the activated fiber. Conditions: sarcomere length 2.15 μ m, 4.0°C, pH 7.0, ionic strength 160 mM, fiber length 5.7 mm, fiber diameter 140 μ m, isometric tension exerted by the activated fiber 92 kN/m^2 , experiment: 04-02-1987.

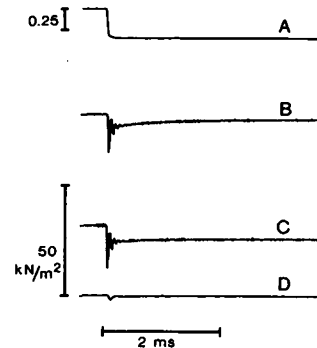


FIGURE 3 Tension transients of a single frog fiber obtained after releases completed within 40 μ s on a 4-ms time scale. The length change is expressed in nanometer/half sarcomere, the tension responses in kN/m^2 . (A) Displacement signal, (B) tension response of the activated fiber, (C) tension response of the rigor fiber, and (D) tension response of the relaxed fiber. Conditions: sarcomere length 2.15 μ m, 4.0°C, pH 7.0, ionic strength 160 mM, fiber length 5.7 mm, fiber diameter 165 μ m, isometric tension of activated fiber: 80 kN/m^2 , rigor fiber: 30 kN/m^2 , experiment: 27-11-1986.

RESULTS

Mechanical Measurements

The initial tension changes denoted as phase 1 and phase 2 (Ford et al., 1977) take place within the first 5–10 ms after applying a length change. This part of tension responses is influenced most by the speed of the length change, as can be seen in Figure 2. Bearing in mind that our interest is focussed on the elastic properties of cross-bridges, we were not only forced to consider the first 5 ms of the tension transients, but also to use quick length changes (completed within 40 μ s) in order to obtain detailed responses.

Tension transients of rigor and activated fibers were considered, because in both states no cross-bridge attachment or detachment occurs within phase 1 and phase 2. Fig. 3 illustrates that these transients look similar within the first 500 μ s and that they tend to deviate only after 1

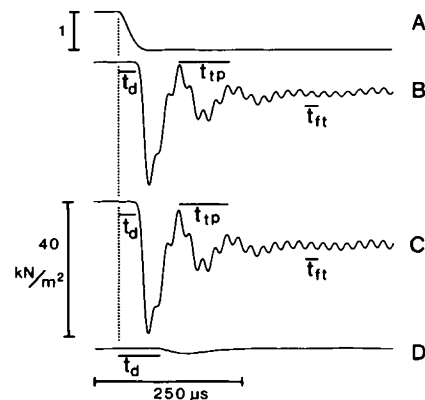


FIGURE 4 The first 500 μ s of tension transients of a single frog fiber to a lengthening completed within 40 μ s. The length change is expressed in nanometer/half sarcomere, the tension responses in kN/m^2 . (A) Displacement signal, (B) tension response of the activated fiber, (C) tension response of the rigor fiber, and (D) tension response of the relaxed fiber. In all traces: t_d - delay between onset displacement and tension response; t_{tp} - oscillation due to transmission phenomena in the fiber; t_n - oscillation due to the force transducer characteristics. Conditions: sarcomere length 2.15 μ m, 4.0°C, pH 7.0, ionic strength 160 mM, fiber length 5.6 mm, fiber diameter 110 μ m, isometric tension of activated fiber: 73 kN/m^2 , rigor fiber: 36 kN/m^2 , experiment: 25-03-1986.

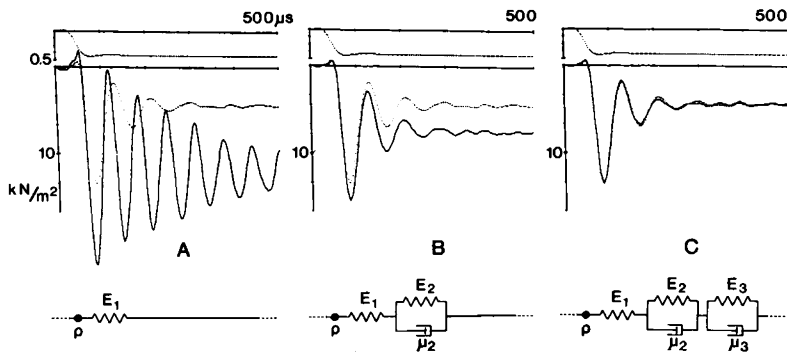


FIGURE 5 Simulation of a tension transient of an activated fiber with three different models. Simulations had to fit in sequence the delay (A); the delay, the tension change during the displacement and the oscillation (B); the delay, the tension change during the displacement, the oscillation and the fast recovery (C). In the simulations the corrections for surrounding fluid and transducer characteristics are included. The small upward deflections at the beginning of the displacement and tension traces are due to the digital filtering. See Methods and Materials with respect to the filter procedure. Note that in A the damping of the oscillation in the simulation is caused by the fluid correction. The measured tension response is corrected for the very slow tension change,

which manifests itself mainly after 500 μ s. (Upper trace) Lengthening of the fiber in nanometer/half sarcomere, (lower traces) tension response and model simulation in kN/m^2 . In all panels, the dotted curve is the measured tension response and the solid curve the simulation with the model shown below. The visco-elastic properties of the half-sarcomere are represented by (A) an undamped elastic element only, (B) an undamped and a damped elastic element in series and (C) an undamped and two damped elastic elements in series according to the model described in Materials and Methods. Conditions: ionic strength 160 mM, pH 7.0, temperature 4.0°C, fiber length 5.0 mm, fiber diameter 125 μ m, isometric tension: 81 kN/m^2 , experiment: 19-09-1985.

ms. The first 500 μ s of tension responses obtained from fibers in the relaxed, rigor, or activated state exhibit the same properties to some extent: a delay, an abrupt tension change, an oscillation, and a fast recovery. The measured delay is the time between the onset of the displacement and tension change, and thus corresponds to the initial transmission velocity of the disturbance in the fiber. Delay measurements, obtained from the same preparation type, were previously published by Stienen and Blangé (1985). The time course of the oscillation in the tension response points to a change in the transmission velocity. Evaluation of the tension responses by the simulation procedure reveals that this difference in transmission velocity is associated with a very fast relaxation time (within microseconds). The fast recovery corresponds with another fast relaxation time. Small oscillations in the tension responses arise from the resonant frequency of the force transducer. In Fig. 4, examples are shown of typical tension responses obtained from a single fiber upon application of a small lengthening of the fiber (1 nm/half sarcomere within 40 μ s).

Fig. 5 illustrates that a model with three visco-elastic elements is a prerequisite for a satisfactory description of the first 500 μ s of tension recording as given in Fig. 4. A tension response of an activated fiber is simulated with three different models. These three models differ only in the number of damped elastic elements. All three models

were used in such a way that they first of all simulated the observed delay and then in sequence the abrupt tension change, the oscillation, and the fast recovery. With a model that consists of an undamped elastic element only, it is impossible to obtain simultaneously the same delay, abrupt change in tension, oscillation, and fast recovery as in the measured response. The model with an undamped and a damped elastic element in series (Blangé and Stienen, 1985b) can account for the delay and the oscillation of the response, but fails to simulate the recovery correctly. The model with five parameters succeeds in describing not only the tension response of activated fibers but also that of relaxed fibers and fibers in rigor (see Fig. 6). Fig. 1 (right) illustrates the small amounts of correction included in the model simulations due to the characteristics of the force transducer and due to the fluid surrounding the fiber. Fig. 1 (left) illustrates the effect of instrumental delays, induced artificially, on the difference between simulated and measured tension responses. In those cases, where the delay between the onset of the displacement and the onset of the measured tension response was deliberately changed by +5 μ s or -5 μ s, the optimal simulation had a considerably greater chi-square value (3 or 10 times) than the situation in which the observed delay was not altered. This confirms the observation that our measurements are not disturbed by instrumental delays.

We confined ourselves to the analysis of tension

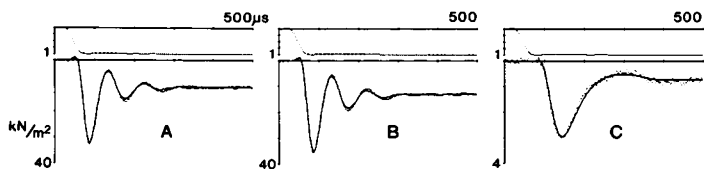


FIGURE 6 Measured and simulated tension responses of a fiber in (A) activation solution, (B) rigor solution and (C) relaxation solution. (All panels, upper trace) displacement (lengthening of the fiber) expressed in nanometer/half sarcomere, (lower trace) tension response (dotted curve) and simulation (solid curve) expressed in kN/m^2 . The small upward deflections at the beginning of the displacement and tension traces are due to the digital filtering. The

response of the activated fiber was just as the responses of rigor and relaxed fibers simulated with the 5-parameter model, except that a correction was made for the slow tension change which manifested itself mainly after 500 μ s. (Conditions) Sarcomere length 2.15 μ m; pH 7.0; ionic strength 160 mM; temperature 4.0°C; fiber length 5.6 mm; fiber diameter 110 μ m; isometric tension activated fiber: 73 kN/m^2 , rigor fiber: 36 kN/m^2 ; experiment: 25-03-1986.

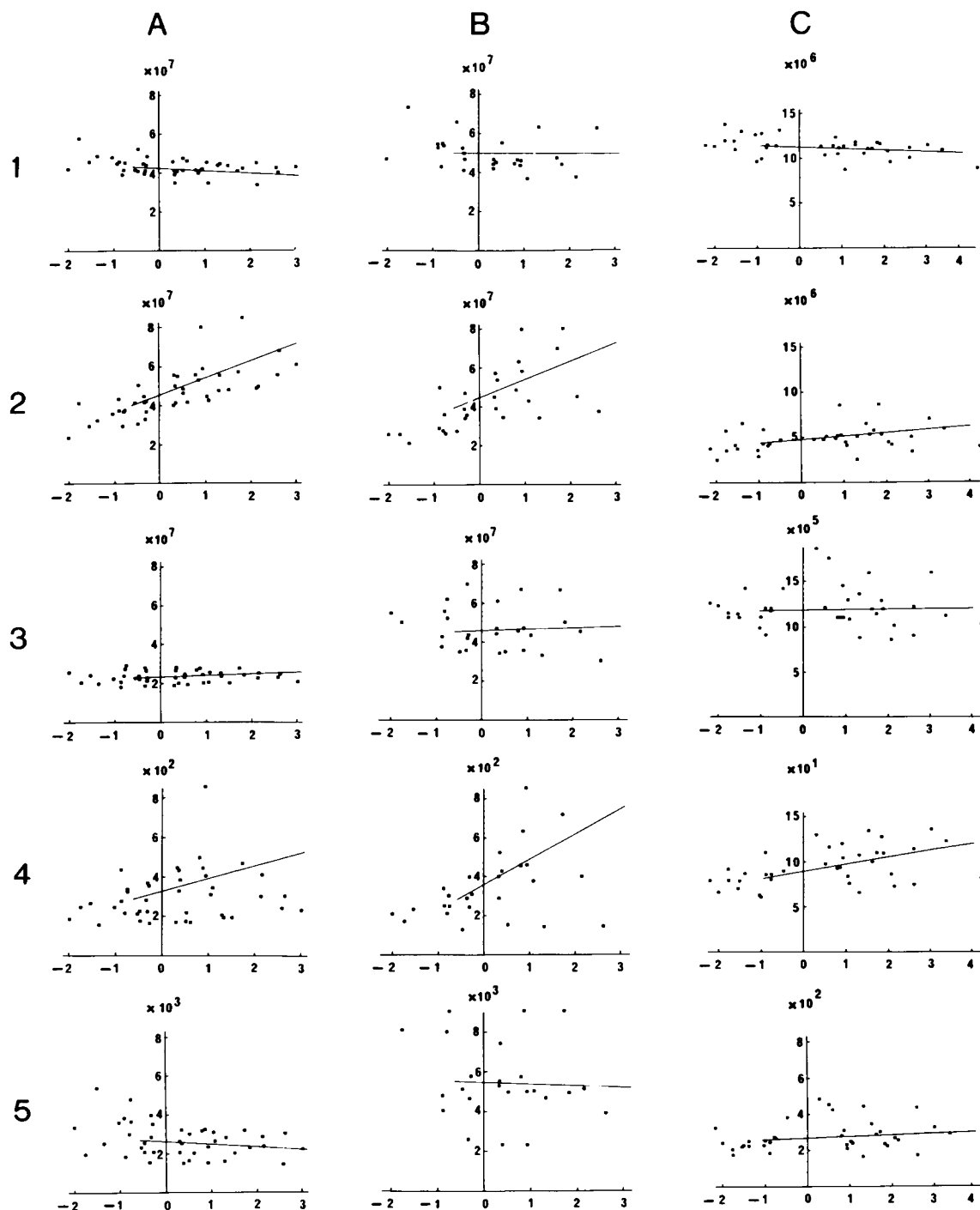


FIGURE 7 A compilation of the estimated five model parameters (necessary to describe the first 500 μ s of tension responses) as a function of the length change. The responses of activated fibers were simulated with the 7-parameter model but only the first five parameters are given. Data obtained from nine single fibers. Conditions as described in Materials and Methods. The horizontal axes are given in nanometer/half sarcomere. The least mean square regression line for each panel is obtained by averaging the least mean square regression lines of all fibers, using only those points which lie between 0.5 nm/half sarcomere (relax: 1.0 nm/half sarcomere) shortening and 3.0 nm/half sarcomere (relax: 4.0 nm/half sarcomere) lengthening. Each point represents the mean of three measurements. Column *A*: the model parameter values of Ca^{2+} -activated fibers — isometric tension: 91 ± 9 kN/m² (mean \pm SEM)-, *B*: rigor fibers — isometric tension: 36 ± 8 kN/m² (mean \pm SEM)- and *C*: relaxed fibers. (*First row*) Undamped elastic element (E_1) in N/m², (*second row*) second elastic element (E_2) in N/m², (*third row*) third elastic element (E_3) in N/m², (*fourth row*) first damping coefficient (μ_2) in Ns/m², and (*fifth row*) second damping coefficient (μ_3) in Ns/m².

responses to small length changes (smaller than 4 nm/half sarcomere), in order to avoid nonlinear behavior (changes of model parameters during the tension response) which would occur according to the known T1, T2 curves (Ford et al., 1977; Stienen and Blangé, 1985). A compilation of results obtained from nine single fibers can be found in Fig. 7. For each of the three fiber conditions (relaxation, rigor and activation), the estimated values of the five model parameters at different length changes are given. Each point in the figure represents the mean of three measurements, and thus three parameter estimates obtained from one fiber. The variation in the estimated parameters was clearly greater for rigor fibers than for activated or relaxed fibers. This especially concerns μ_2 , μ_3 , and E_3 . The variation in the parameters of the rigor fibers did not correlate with external conditions like rigor tension, fiber diameter, or fiber length. Only those estimated parameter values which were acquired from measurements between a shortening of 0.5 nm/half sarcomere (relax: 1.0 nm/half sarcomere) and a lengthening of 3.0 nm/half sarcomere (relax: 4.0 nm/half sarcomere) were used to calculate a least mean square regression line. The parameter estimate beyond this range, especially the shortenings larger than 1.5 nm/half sarcomere, appeared to be less reliable because of a less good fit of the tension responses to the model. The least mean square regression lines, drawn in Fig. 7, were obtained by averaging the regression lines of the nine individual fibers for each parameter.

It can be seen that the regression lines of E_2 and μ_2 are sloped and the estimates of these parameters appear to depend on the applied length change (confidence level 1%). This nonlinear behavior of the fibers cannot unambiguously be ascribed to the model elements E_2 and μ_2 only, because our method is based on the assumption that the fiber segment responds linearly with respect to the amplitude of length change. Although small exchanges between E_1 and E_2 cannot be excluded, it is likely that at least part of this behavior is due to the characteristic of E_2 and μ_2 .

In order to compare the elastic elements and damping coefficients in the three conditions, notwithstanding the dependence on the length change of some parameters, we used the parameter estimates, which followed from the regression lines at zero displacement. Table IIA gives an overview of these parameter values of rigor, relaxed, and activated fibers. The first three parameters of rigor and activated fibers (E_1 , E_2 , and μ_2) do not differ (confidence level 1%).

The arrangement of elastic elements in our model is not unique. To obtain a representation which is independent of the specific arrangement of these elements we transformed the five model parameters into two recovery components with different time constants. As follows from the elastic impedance,

$$1/Z(s) = 1/E_1 + 1/(E_2 + \mu_2 s) + 1/(E_3 + \mu_3 s) \quad (6)$$

the behavior of the elastic model unit (neglecting the

TABLE II
MODEL PARAMETERS OF FREEZE-DRIED SINGLE FIBERS

A	Activation	Rigor	Relax	
E_1	4.29 ± 0.09	4.93 ± 0.29	1.13 ± 0.03	*10 ⁷
E_2	4.53 ± 0.27	4.46 ± 0.47	0.47 ± 0.04	*10 ⁷
E_3	2.32 ± 0.09	4.50 ± 0.47	0.12 ± 0.01	*10 ⁷
μ_2	3.19 ± 0.48	3.63 ± 0.65	0.87 ± 0.06	*10 ²
μ_3	2.68 ± 0.23	5.50 ± 0.98	0.27 ± 0.03	*10 ³
B				
v_{tr}	2.01 ± 0.02	2.16 ± 0.06	1.03 ± 0.01	*10 ²
τ_1	3.50 ± 0.41	3.79 ± 0.52	4.63 ± 0.24	
E_{app2}	2.18 ± 0.07	2.26 ± 0.12	0.33 ± 0.02	*10 ⁷
τ_2	6.12 ± 0.45	8.19 ± 0.92	7.20 ± 0.54	*10 ¹
E_{app3}	1.12 ± 0.02	1.49 ± 0.09	0.09 ± 0.01	*10 ⁷

(A) Mean values of the five model parameters obtained from the least mean square regression lines from the data presented in Fig. 7. The mean and standard error of the mean are given for relaxed, activated, and rigor fibers. E_1 , E_2 , and E_3 in N/m²; μ_2 and μ_3 in Ns/m².

(B) Alternative representation of the values of the five model parameters from Table IIA. Transmission velocity of the displacement through the fiber (v_{tr}) in m/s; apparent elastic constants E_{app2} and E_{app3} in N/m²; time constants τ_1 and τ_2 in μ s. Conditions: 40°C, pH 7.0, ionic strength 160 mM, sarcomere length 2.15 μ m, nine fibers.

density in the unit) to an instantaneous length change can be described with an instantaneous change to a first tension level, a recovery with a time constant τ_1 to a second tension level, and finally a second recovery with a time constant τ_2 to a third tension level. The three tension levels denote the final tension, that was reached if respectively only E_1 , $E_1 + E_2$, or $E_1 + E_2 + E_3$ would be present. The three corresponding apparent elastic constants are defined by:

$$E_{app1} = E_1 \quad (7)$$

$$(E_{app2})^{-1} = (E_1)^{-1} + (E_2)^{-1} \quad (8)$$

$$(E_{app3})^{-1} = (E_1)^{-1} + (E_2)^{-1} + (E_3)^{-1}. \quad (9)$$

This representation of the results can be found in Table IIB. The undamped elastic element (E_1) corresponds with a transmission velocity of the displacement through the fiber. In activation and rigor, this velocity is ~200 m/s, while in relaxed fibers a value of ~100 m/s is obtained.

E_{app2} is equal within 5% for activated and rigor fibers, whereas during activation E_{app3} is $\frac{3}{4}$ of the corresponding rigor value. The time constants do not differ. The apparent elastic constants E_{app2} and E_{app3} of relaxed fibers are much smaller than those of the activated or rigor fibers. The time constants in relaxed fibers do not differ from those in the other two conditions (1% level).

In Table III, the model parameter estimates of Triton skinned fibers is presented. Obviously, the same elastic components were present as in the freeze-dried fibers, although the values, obtained with these preparations, differ slightly. However, due to the difficulties with fiber mounting (see Methods and Materials), the parameter estimates were less accurate than those obtained with freeze-dried fibers. Optimal simulations in case of acti-

TABLE III
MODEL PARAMETERS OF TRITON-TREATED SINGLE FIBERS

A	Activation	Rigor	Relax	
E_1	3.79 ± 0.27	4.31 ± 0.11	0.80 ± 0.14	$*10^7$
E_2	4.77 ± 1.48	4.55 ± 0.34	0.27 ± 0.04	$*10^7$
E_3	2.63 ± 0.22	3.87 ± 0.37	0.03 ± 0.01	$*10^7$
μ_2	2.15 ± 1.04	4.44 ± 0.35	0.38 ± 0.05	$*10^2$
μ_3	2.07 ± 1.03	3.97 ± 0.16	0.09 ± 0.01	$*10^3$
B				
v_{tr}	1.89 ± 0.07	2.02 ± 0.03	0.87 ± 0.08	$*10^2$
τ_1	2.47 ± 0.74	4.87 ± 0.31	2.83 ± 0.06	
E_{app2}	2.16 ± 0.41	2.21 ± 0.16	0.20 ± 0.04	$*10^7$
τ_2	5.79 ± 0.88	6.71 ± 0.25	4.87 ± 0.71	$*10^1$
E_{app3}	1.16 ± 0.15	1.40 ± 0.12	0.02 ± 0.01	$*10^7$

Mean values of model parameters obtained from two chemically-skinned (Triton treated) fibers. Isometric tension activated fibers: 110 ± 5 kN/m², rigor fibers: 40 ± 5 kN/m² (mean \pm SEM). For further explanation and experimental conditions see the legend of Table II.

activated and rigor fibers required a different virtual fiber length than in case of relaxed fibers. For instance, the virtual fiber length in case of relaxed fibers corresponded with the visible fiber length free of glue, whereas the virtual fiber length of activated/rigor fibers exceeded this visible free-fiber length with 15%. This suggests a significant influence of the mounting procedure on the elasticity measurements. The relaxed Triton fibers were to some extent (E_{app3}) less stiff than the relaxed freeze-dried fibers.

Fig. 8 illustrates that in activated fibers a recovery component is present with a much slower time constant than the ones mentioned so far. Using the 7-parameter model it is possible to describe the tension transients of Ca²⁺ activated fibers up to the first 2.0 (or 5.0) ms. Such a slow recovery could not unambiguously be resolved from the tension transients of rigor or relaxed fibers. The activated fibers recovered from the third apparent elastic constant E_{app3} (mean \pm SEM: $1.12 \pm 0.07 * 10^7$ N/m²) to a fourth apparent elastic constant E_{app4} (mean \pm SEM: $0.50 \pm 0.08 * 10^7$ N/m²) with a time constant τ_3 of 1.04 ± 0.14 ms.

The four apparent tension levels, which correspond to the apparent elastic constants necessary to describe the

first 5 ms of activated freeze-dried fibers, can be expressed as a percentage of isometric tension which allows us to compare these results in Fig. 9 with T_1/T_0 and T_2/T_0 curves of intact (Ford et al., 1977) and freeze-dried fibers (Stienen and Blangé, 1985). T_1/T_0 and T_2/T_0 curves of freeze-dried fibers (obtained from responses after a 150- μ s step) and intact fibers (obtained from responses after a 200 μ s step) are comparable. It is furthermore obvious that the apparent elastic constant E_{app2} of activated freeze-dried fibers corresponds to T_1/T_0 , whereas E_{app4} corresponds to T_2/T_0 .

X-ray Measurements

Typical examples of analyzed diffraction patterns, after the procedure described, are presented in Fig. 10. In Table IV the estimated d_{10} , I_{11}/I_{10} , and A/M values obtained from data of eight fibers and two bundles are summarized.

The d_{10} value of relaxed fibers is comparable with the one found in mechanically-skinned fibers (Matsubara et al., 1984) and more than the value found in intact frog muscles (Yu et al., 1985). The intensity ratio I_{11}/I_{10} increases from relaxation, activation to rigor, just as found in intact frog muscle (Haselgrove and Huxley, 1973). However, the intensity ratio I_{11}/I_{10} of relaxed fibers is almost twice the value obtained from other preparations (Yu et al., 1985; Brenner et al., 1984). The calculated mass ratio A/M of relaxed fibers is 1.5 times the ratio found in intact frog muscles (Haselgrove and Huxley, 1973). The observation that freeze-dried relaxed fibers were stiffer than the chemically-skinned (Triton treated) fibers might be correlated with this increased amount of mass near the actin filament or with a different filament spacing (Goldman and Simmons, 1986).

The intensity ratio I_{11}/I_{10} and distance d_{10} of activated and rigor fibers are similar to those found by Yu et al. (1985), Brenner et al. (1984), and Matsubara et al. (1984). The mass ratio of A/M of activated and rigor fibers is similar to the values found by Haselgrove and Huxley (1973). The same applies to the calculated mass shift towards the actin filament when the fiber is activated. This shift is 49% (low value) or 47% (high value) of the mass shift which occurs when the fiber goes into rigor.

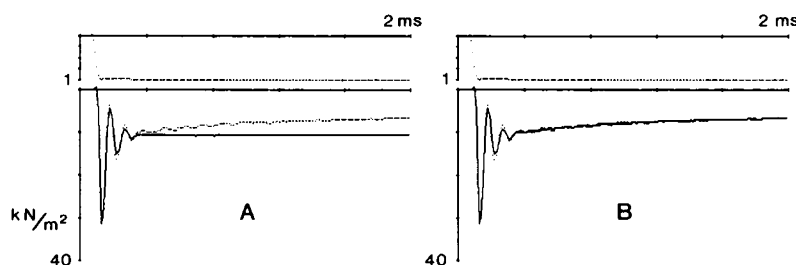


FIGURE 8 For simulation of tension transients of Ca²⁺-activated fibers over the first 2 ms an extra damped elastic element is needed in addition to the undamped and two damped elements. (Upper traces) Displacement (lengthening of the fiber), (lower traces) tension response and model-simulation. All traces were digitally filtered. Conditions as mentioned in Fig. 4. Experiment: 25-03-1986. (A) Measured tension response (dotted curve) and simulation obtained with the 5-parameter model (solid curve). (B) same as in A, but simulation obtained with the 7-parameter model.

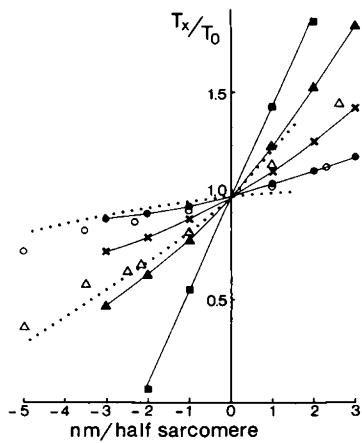


FIGURE 9 T_1/T_0 and T_2/T_0 curves (dotted curves) of activated intact frog muscle fibers, length changes completed within 200 μ s, temperature 3.7°C. (Ford et al., 1977 Fig. 32); T_1/T_0 (open triangles) and T_2/T_0 (open circles) of freeze-dried frog muscle fibers, length changes completed within 150 μ s, temperature 2.5°C. (Stienen and Blangé 1985 Fig. 4); T_{app1}/T_0 (filled squares), T_{app2}/T_0 (filled triangles), T_{app3}/T_0 (crosses), and T_{app4}/T_0 (filled circles) of activated freeze-dried frog muscle fibers, length change completed within 40 μ s, temperature 4.0°C. T_{appx} corresponds with the apparent elasticities E_{appx} times the applied length change. E_{appx} were obtained from the data given in Fig. 7. Experimental conditions as given in Fig. 7.

DISCUSSION

Freeze-dried fibers have been used in the study of the contraction mechanism for several years (Blangé and Stienen, 1985b; Stienen et al., 1983; Stienen and Blangé, 1985; Stienen et al., 1985; van der Laarse et al., 1986). This type of preparation appeared to be suitable for experiments with very fast length changes. Other types of measurements, like ATPase activity, Ca^{2+} sensitivity, isometric force, electron micrographs, and x-ray diffraction patterns of activated, relaxed, and rigor fibers, indicate that this type of preparation has characteristics that are within the range of results that one can expect from skinned fibers. In order to exclude the possibility that the phenomena which were observed during the first 500 μ s of the tension responses of activated, relaxed, and rigor fibers were due to the preparation procedure, the results of two

experiments with chemically-skinned fibers have been included. In both types of preparations we observed the fast recovery phenomena. These fast recovery components were also observed in intact fibers (van den Hooff and Blangé, 1984). All the above mentioned results indicate that the freeze-dried fiber preparation is a suitable model system for the present studies.

The first 5 ms of tension responses of activated fibers contain recovery components, which can be separated into four corresponding apparent elastic levels and three recovery times between these levels. The second level corresponds with values of the T_1 curve, whereas the fourth level corresponds with values of the T_2 curve. The T_1 and T_2 curves of freeze-dried fibers (Stienen and Blangé, 1985) are rather similar to the T_1 and T_2 curves of intact fibers (Ford et al., 1977).

The value of the first apparent elastic constant (identical with E_1) of activated fibers is comparable with the one mentioned by Stienen and Blangé (1985). In their study, the undamped elastic element was calculated from the measured delay between the onset of the tension response and the start of the displacement as function of fiber length. The small deviation that was observed is due to different methods of analyzing the measurements.

The fastest time constant (4 μ s), present in activated fibers, was already observed by Blangé and Stienen (1985b), although their estimates were less accurate by lack of an optimizing fitting procedure. The same applies to the preliminary estimates of the second recovery time (70 μ s) (Blangé and Stienen, 1985a). Their value of the second time constant was overestimated because the influence of the third (1 ms) time constant was neglected.

Kawai and Brandt (1980) resolved three exponential rate processes from the complex stiffness of activated muscle fibers. All three were absent in rigor and relaxed fibers. The fastest rate constant was close to our slowest time constant (1 ms). The 1-ms time constant, which was only present in activated fibers, corresponds to the recovery half-time mentioned by Ford et al. (1977). Harrington (1979) tried to correlate this recovery half-time constant with an helix-coil transition. Eisenberg et al. (1980) accounted for the recovery half-time by assuming that this reflected the force-generating step in the cross-bridge

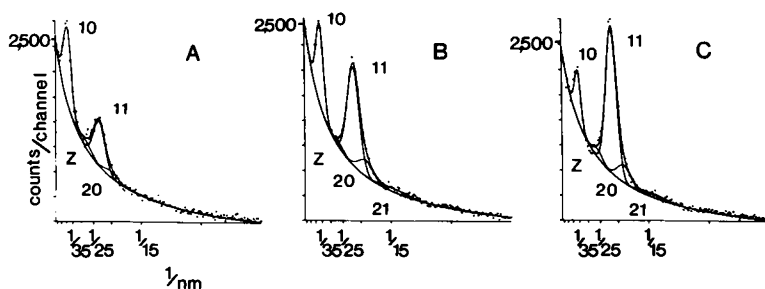


FIGURE 10 Typical equatorial x-ray diffraction patterns of freeze-dried single fibers. In each panel the measured scattering pattern (dotted curve) and the least square fit (solid curve) is shown. The calculated individual peaks (10, 11, 20, 21, and Z-line) are also drawn (solid curves). The measured patterns were corrected for detector characteristics and scattering due to the mica windows of the measuring cells. The background of the patterns arises from the fiber. (A) Pattern obtained from a relaxed single fiber (B) from the activated fiber (isometric tension 76 kN/m²) and (C) from the rigor fiber (isometric tension 34 kN/m²). Conditions as in the mechanical experiments. Experiment: 20-09-1986.

TABLE IV
 d_{10} , I_{11}/I_{10} , AND A/M OF FREEZE-DRIED SINGLE FIBERS

	Activation	Rigor	Relax
d_{10}	38.3 ± 0.3	38.3 ± 0.1	40.4 ± 0.3
I_{11}/I_{10}	1.7 ± 0.1	3.8 ± 0.3	1.0 ± 0.03
A/M(low)	0.265 ± 0.011	0.426 ± 0.017	0.170 ± 0.010
A/M(high)	0.429 ± 0.009	0.533 ± 0.013	0.354 ± 0.008

Mean and standard error of the mean of the intensity ratio I_{11}/I_{10} , the mass ratio A/M and the d_{10} distance of activated, relaxed, and rigor fiber bundles and single fibers. d_{10} in nanometer. A/M(low) and A/M(high) refer to different positions of the background (see Materials and Methods). Data obtained from eight single fibers and two bundles. Conditions as in the mechanical experiments. Experiments: 25-01-1986, 26-01-1986, 20-09-1986, 24-09-1986, and 27-09-1986.

cycle. This would correspond to a transition between $AM^+ \cdot ADP \cdot P_i$ and $AM \cdot ADP$.

The value of the first apparent elastic constant E_{app1} (which is identical with the undamped elastic element E_1) in relaxed fibers is comparable with those found by Blangé and Stienen (1985b) and Stienen and Blangé (1985). The transmission velocity (which corresponds to E_1) of our relaxed fibers is also in agreement with the results found by Schoenberg et al. (1974). The apparent elastic constants E_{app2} and E_{app3} of relaxed fibers were up to twenty times smaller compared with those of activated or rigor fibers. The third apparent elastic constant (E_{app3}) of relaxed fibers is comparable with the elastic modulus in resting intact frog fibers (Lännergren 1971). Goldman and Simmons (1986) observed an increase of stiffness in relaxed mechanically-skinned fibers as function of filament spacing. Their low stiffness value (10–30 kN/m² at 0 g PVP-40/l and 300–500 kN/m² at 40 g PVP-40/l; ionic strength of solutions: 200 mM) should be compared with our E_{app3} value. The filament spacing of our relaxed freeze-dried fibers is intermediate between the spacings of mechanically-skinned fibers at 0 g PVP-40/l and 40 g PVP-40/l. This observation, together with the observation that stiffness of relaxed fibers depends on the ionic strength of the incubation solution (manuscript in preparation), can at least partly account for the observed higher stiffness. The small deviations which we observed between the apparent elasticities of freeze-dried fibers and Triton-treated fibers could be due to differences in filament spacings. Differences in passive structures due to preparing methods can not be excluded.

The fastest two time constants (4 and 70 μ s) are present in the activated and rigor state as well as in the relaxed state. This could point to cross-bridge activity in all three states, if the observed time constants have their origin in cross-bridge properties, or in effects due to viscous drag between the filaments. If these time constants have their sole origin in drag, then it is hard to explain the difference in damping coefficient μ_2 in the case of relaxed compared with activated/rigor fibers and the differences in damping

coefficient μ_3 in all the three states. Filament spacing might have effects on viscous damping and thus influence the damping coefficients. This could explain part of the differences between activated/rigor fibers and relaxed fibers with respect to the damping coefficients. On the other hand, it certainly cannot explain the differences between rigor and activated fibers with respect to the damping coefficient μ_3 , which makes it likely that the differences between activated and rigor fibers are reflections of cross-bridge behavior. In summary, although effects due to drag cannot be excluded, it seems unlikely that these effects are predominant in case of activated and rigor fibers. Finally, we cannot exclude faster time constants than 4 μ s.

The value of the immediate stiffness (E_1) of relaxed fibers, which is ~25% of the immediate stiffness of rigor or activated fibers, would point to a high number of cross-bridges in the relaxed fiber under normal ionic strength conditions (160 mM) if this stiffness is caused by cross-bridge numbers only. However, it remains doubtful whether E_1 , in activating, relaxing, and rigor conditions, is an unbiased measure of cross-bridge numbers. There is, according to Blangé et al. (1985), no linear relationship between E_1 and active isometric tension which suggests that only part of the compliance has its origin in cross-bridges. We noticed that all the model parameters of relaxed fibers are more or less sensitive to filament spacing changes induced by osmotic compression (manuscript in preparation). Especially E_1 depended on changes in filament spacing which suggests that E_1 of relaxed fibers is, at least partly, caused by phenomena different from the number of cross-bridges. We cannot exclude that weakly-attached cross-bridges are present in relaxed frog muscle fibers at 160-mM ionic strength. However, more detailed knowledge of the changes in the parameter values of relaxed fibers as a function of ionic strength is needed in order to obtain an estimate of the number of weakly-attached cross-bridges.

Stiffness measurements of activated and rigor fibers have been used for a first impression of the number of cross-bridges in both states (Yamamoto and Herzig, 1978; Goldman and Simmons, 1977). It is reasonable to compare elastic constants in both states, because filament spacing is identical in case of activated and rigor fibers. Stiffness differences cannot be attributed to different filament spacing. Comparing stiffness of activated and rigor fibers should be restricted to the first three apparent elastic constants, because of absence of the 1 ms time constant in rigor.

Yamamoto and Herzig (1978) found that stiffness of activated fibers is $\frac{3}{4}$ of rigor stiffness. They used slow displacements (completed within 700 μ s), which means that their T_1/T_0 value cannot be compared with the one from Ford et al. (1977) and thus not with our second apparent elastic constant. Their result would be in agreement with our results if their T_1/T_0 and our E_{app3} are

equivalent quantities. Goldman and Simmons (1977) compared T_1 curves of rigor and activated fibers (using displacements completed within 200 μ s), which also resulted in a ratio of $\frac{3}{4}$. As we have shown, T_1 curves of activated fibers obtained with these fast displacements correspond to our second apparent elastic constant (E_{app2}). When we compare this elastic constant of activated and rigor fibers, we obtain no differences. However, these results cannot unambiguously be compared with each other, because their results were obtained with 200 mM ionic strength incubation solutions. Rigor stiffness as well as stiffness of activated fibers depends on the ionic strength of the solutions (manuscript in preparation).

We have shown that compliance of the muscle fiber in rigor consists of three components, which are found as well during activation. E_{app2} appears to be the same within 5% during rigor and activation and E_{app1} is the same within 15%. During activation the value of E_{app3} is 75% of that during rigor. The question which of these apparent elastic constants can be used as a measure of the relative number of cross-bridges in the rigor and activated state, assuming the same stiffness per cross-bridge in both states, remains to be answered. Ford et al. (1981) stated that in intact activated fibers ~80%, but probably well over 90%, of the measured instantaneous compliance is attributable to cross-bridges. They concluded that instantaneous stiffness, which corresponds in their experiments with T_1 , can be used as a measure of the number of cross-bridges. We argued that in skinned fibers T_1 corresponds with E_{app2} . The question arises whether the immediate elastic constant (E_{app1}) that we observed is a measure of the number of cross-bridges. Preliminary results (Blangé et al., 1985) of stiffness measurements of activated fibers as function of Ca^{2+} concentration of the incubation solution suggest that the immediate compliance is only partly located in the cross-bridges, which leaves only E_{app2} and E_{app3} as possible candidates for a measure of number of cross-bridges. Although, according to the equatorial reflections of activated and rigor fibers, the amount of mass-shift during activation is only ~50% of that in rigor, one could try to explain the similarity of E_{app2} during rigor and activation by assuming the same number of cross-bridges in both states with on average the same stiffness per cross-bridge. However, one has then to assume that E_{app3} or overall compliance of the rigor cross-bridge is higher than the overall compliance of the cross-bridge during activation, in order to explain the difference in E_{app3} . This may be a realistic hypothesis, but it repudiates that similarity of E_{app2} is due to equal numbers of cross-bridges in both states. This argument applies also to the similarity of E_{app1} during rigor and activation.

Two possibilities are left to explain the proportions of the corresponding apparent stiffnesses in rigor and during isometric activation. First, the visco-elastic properties of cross-bridges can be different during rigor and activation. This possibility leads to the conclusion that it is impossible

to deduce relative numbers of attached cross-bridges from stiffness measurements of rigor and activated fibers. Secondly, the number of cross-bridges during activation relative to the number in rigor can be 75% or less. In this case tension dependence could explain the relatively high value of E_{app2} (and E_{app1}) during activation. The figure of 75% is based on proportionality of E_{app3} with cross-bridge numbers. If E_3 , instead of E_{app3} , is assumed to be proportional to cross-bridge numbers, the relative number would be 50% rather than 75%. This leads to the conclusion that E_1 (equals E_{app1}) and E_2 are not unambiguously correlated with cross-bridge numbers. Tension dependence of E_2 could explain why the value of this parameter in rigor fibers equals the value in activated fibers. The amount of mass-shift is in agreement with a relative number of cross-bridges of 75% or less.

As noted, it cannot be excluded that the elastic properties of cross-bridges are different during rigor and activation. Results from electron paramagnetic resonance spectroscopy measurements (Cooke et al., 1982), which lead to the conclusion that rigor cross-bridges are highly ordered whereas cross-bridges in activated fibers display (at least at some structural parts) a nonrigid behavior, are compatible with differences in elastic properties. Results from caged-ATP measurements (Goldman et al., 1984) suggest that in activated psoas fibers the AM state is hardly occupied. On the other hand the AM state is the only state occupied in case of rigor.

More detailed knowledge, than available at this moment, about visco-elastic properties of muscle fibers in the submillisecond time domain, expressed in undamped and damped elastic elements, is needed to decide between the above mentioned two possibilities.

We thank Dr. C. Nave and Dr. H. Gerritsen (Synchrotron Radiation Source Daresbury) for assistance during the x-ray measurements, Dr. G. J. M. Stienen for advice on fiber preparing methods, Mr. A. W. Schreurs and Mr. P. Broekhuijsen for technical assistance.

This study was supported by the Netherlands Organization for the Advancement of Pure Research (Z.W.O.) also in connection with the agreement between the Science and Engineering Research Council and Z.W.O. concerning the Synchrotron Radiation Source.

Received for publication 2 July 1987 and in final form 18 April 1988.

REFERENCES

- Blangé, T., and G. J. M. Stienen. 1985a. The early part of the tension transient of activated skinned muscle fibres of the frog at high time-resolution. *J. Physiol. (Lond.)* 366:74.
- Blangé, T., and G. J. M. Stienen. 1985b. Transmission phenomena and early tension recovery on skinned muscle fibres of the frog. *Pfluegers Arch. Eur. J. Physiol.* 405:12-18.
- Blangé, T., G. J. M. Stienen, and B. W. Treijtel. 1985. Active stiffness in frog skinned muscle fibres at different Ca concentrations. *J. Physiol. (Lond.)* 366:77.
- Brenner, B., L. C. Yu, and R. J. Podolsky. 1984. X-ray diffraction evidence for cross-bridge formation in relaxed muscle fibers at various ionic strengths. *Biophys. J.* 46:299-306.

- Cooke, R., M. S. Crowder, and D. D. Thomas. 1982. Orientation of spin labels attached to cross-bridges in contracting muscle fibres. *Nature (Lond.)* 300:776-778.
- Eisenberg, E., T. L. Hill, and Y. Chen. 1980. Cross-bridge model of muscle contraction. Quantitative analysis. *Biophys. J.* 29:195-227.
- Fabiato, A., and F. Fabiato. 1979. Calculator programs for computing the composition of the solutions containing multiple metals and ligands used for the experiments in skinned muscle cells. *J. Physiol. (Paris)* 75:463-505.
- Ford, L. E., A. F. Huxley, and R. M. Simmons. 1974. Mechanism of early tension recovery after a quick release in tetanized muscle fibres. *J. Physiol. (Lond.)* 240:42-43.
- Ford, L. E., A. F. Huxley, and R. M. Simmons. 1977. Tension responses to sudden length change in stimulated frog muscle fibres. *J. Physiol. (Lond.)* 269:441-515.
- Ford, L. E., A. F. Huxley, and R. M. Simmons. 1981. The relation between stiffness and filament overlap in stimulated frog muscle fibres. *J. Physiol. (Lond.)* 311:219-249.
- Godt, R. E., and B. D. Lindley. 1982. Influence of temperature upon contractile activation and isometric force production in mechanically skinned muscle fibres of the frog. *J. Gen. Physiol.* 80:279-297.
- Goldman, Y. E., and R. M. Simmons. 1977. Active and rigor muscle stiffness. *J. Physiol. (Lond.)* 269:55-57.
- Goldman, Y. E., and R. M. Simmons. 1986. The stiffness of frog skinned muscle fibres at altered lateral filament spacing. *J. Physiol. (Lond.)* 378:175-194.
- Goldman, Y. E., M. G. Hibberd, and D. R. Trentham. 1984. Relaxation of rabbit psoas muscle fibres from rigor by photochemical generation of adenosine-5'-triphosphate. *J. Physiol. (Lond.)* 354:577-604.
- Harrington, W. F. 1979. On the origin of contractile force in skeletal muscle. *Proc. Natl. Acad. Sci. USA* 76:5066-5077.
- Haselgrove, J. C., and H. E. Huxley. 1973. X-ray evidence for radial cross-bridge movement and for the sliding filament model in actively contracting skeletal muscle. *J. Mol. Biol.* 77:549-568.
- Hooff, H. van den, and T. Blangé. 1984. Superfast tension transients from intact muscle fibres. *Pfluegers Arch. Eur. J. Physiol.* 400:280-285.
- Hooff, H. van den, T. Blangé, and L. H. van der Tweel. 1982. A displacement servosystem for muscle research permitting 50 μm length changes within 40 μs . *Pfluegers Arch. Eur. J. Physiol.* 395:152-155.
- Kawai, M., and P. W. Brandt. 1980. Sinusoidal analysis: a high resolution method for correlating biochemical reactions with physiological processes in activated skeletal muscles of rabbit, frog and crayfish. *J. Muscle Res. Cell Motil.* 1:279-303.
- Laarse, W. J. van der, P. C. Diegenbach, and M. A. Hemminga. 1986. Calcium-stimulated myofibrillar ATPase activity correlates with shortening velocity of muscle fibres in *Xenopus laevis*. *Histochem. J.* 18:487-496.
- Lännergren, J. 1971. The effect of low-level activation on the mechanical properties of isolated frog muscle fibres. *J. Gen. Physiol.* 62:737-755.
- Magid, A., and M. K. Reedy. 1980. X-ray diffraction observations of chemically-skinned frog skeletal muscle processed by an improved method. *Biophys. J.* 30:27-40.
- Matsubara, I., Y. E. Goldman, and R. M. Simmons. 1984. Changes in the lateral filament spacing of skinned muscle fibres when cross-bridges attach. *J. Mol. Biol.* 173:15-33.
- McClellan, J. H., T. W. Parks, and L. R. Rabiner. 1973. A computer program for designing optimum FIR linear phase digital filters. *IEEE (Inst. Electr. Electron. Eng.) Trans. Biomed. Eng.* 6:506-526.
- Moiescu, D. G., and R. Thieleczek. 1978. Calcium and strontium concentration changes within skinned muscle preparations following a change in external bathing solution. *J. Physiol. (Lond.)* 275:241-262.
- Nave, C., J. R. Helliwell, P. R. Moore, A. W. Thompson, J. S. Worgan, R. J. Greenall, A. Miller, S. K. Burtley, J. Bradshaw, W. J. Pigram, W. Fuller, D. P. Siddons, M. Deutsch, and R. T. Tregear. 1985. Facilities for solution scattering and fibre diffraction at the Daresbury SRS. *J. Appl. Cryst.* 18:396-403.
- Schoenberg, M., J. B. Wells, and R. J. Podolsky. 1974. Muscle compliance and the longitudinal transmission of mechanical impulses. *J. Gen. Physiol.* 64:623-642.
- Stienen, G. J. M., and T. Blangé. 1985. Tension responses to rapid length changes in skinned muscle fibres of the frog. *Pfluegers Arch. Eur. J. Physiol.* 405:5-11.
- Stienen, G. J. M., K. Güth, and J. C. Rüegg. 1983. Force and force transients in skeletal muscle fibres of the frog skinned by freeze-drying. *Pfluegers Arch. Eur. J. Physiol.* 397:272-276.
- Stienen, G. J. M., T. Blangé, and B. W. Treijtel. 1985. Tension development and calcium sensitivity in skinned muscle fibres of the frog. *Pfluegers Arch. Eur. J. Physiol.* 405:19-23.
- Yamamoto, T., and J. W. Herzig. 1978. Series elastic properties of skinned muscle fibres in contraction and rigor. *Pfluegers Arch. Eur. J. Physiol.* 373:21-24.
- Yu, L. C., A. C. Steven, G. R. S. Naylor, R. C. Gamble, and R. J. Podolsky. 1985. Distribution of mass in relaxed frog skeletal muscle and its redistribution upon activation. *Biophys. J.* 47:311-321.